CHAPTER SEVENTY SIX

A Numerical Model For Refraction Of Linear And Cnoidal Waves

John R. Headland[1], A.M. ASCE
Hsiao-Ling Chu[2], M. ASCE

Abstract

A numerical model for refraction of linear and cnoidal waves over an arbitrary bottom is presented. The model, which is based on the ray theory of refraction (11), utilizes linear theory in deep and intermediate water and cnoidal theory in shallow water. The model permits one to determine nearshore wave properties using a nonlinear wave theory. Nearshore wave properties such as wave height, celerity, and wave angle determined using the linear-cnoidal refraction model may vary considerably from those determined using a linear refraction model. In general, cnoidal waves refract less, travel faster, and shoal higher than linear waves. This result can have a considerable effect on coastal engineering design, particularly in the areas of coastal structure design and longshore transport computations.

Introduction

Linear theory is generally used for wave shoaling and refraction computations despite its well-documented inability to accurately predict shallow water wave characteristics (6). Several investigators (6, 8, 14) have used nonlinear theories to analyze wave refraction over straight and parallel bottom contours but have not extended the work to an arbitrary bottom. Crowley et. al. (5) have developed a nonlinear refraction model for an arbitrary bottom utilizing vocoidal wave theory. This paper presents a numerical model for wave refraction over an arbitrary bottom which incorporates linear theory in deep and intermediate water but uses cnoidal theory in shallow water.

The numerical model presented herein is based on the ray theory of refraction. Ray theory suffers from several shortcomings, especially the inability to provide realistic solutions in areas of strong convergence and caustics. A variety of refraction-diffraction models have been developed in recent years (1, 2, 12) to overcome problems associated with ray theory. These models may utilize either linear (2, 12) or nonlinear theory (1). Refraction-diffraction models are clearly an improvement over ray theory, but use of these models requires substantial computer time even for a

[1]Coastal Engineer, Moffatt and Nichol Engineers, Suite 107, 3717 National Drive, Raleigh, North Carolina 27612 and Graduate Student, [2]Department of Civil Engineering, Duke University, Durham, NC 27706.
[2]Professor of Civil Engineering, California State University, Long Beach, California 90840.

relatively small geographical area (2). Ray models are therefore indispensible at the present state-of-the-art and are often used as input to a refraction-diffraction model or to a physical model. Ray models were recently used on two major coastal engineering projects (9, 10).

The objective of this paper is to present the governing equations for wave refraction, present the linear and cnoidal equations used in them, and discuss their numerical solution. Application of the model to straight and parallel bottom contours and an idealized shoal are presented and discussed. Differences in nearshore wave characteristics based on cnoidal versus linear wave refraction are emphasized.

Wave Refraction Equations

Figure 1 illustrates the nomenclature and coordinate system for the wave refraction problem. The wave ray (orthogonal) travels with celerity, c, makes an angle, A, with the x-axis, and its position at a given time, t, is defined by the coordinates, x, and y. The wave ray separation faction, β, which is related to the refraction coefficient by $K = \sqrt{1/\beta}$, is also defined in Figure 1. The governing equations for wave refraction used in the model are those presented by Skovgaard et. al. (13) with time, t, as the independent variable. Wave ray paths are governed by the following equations:

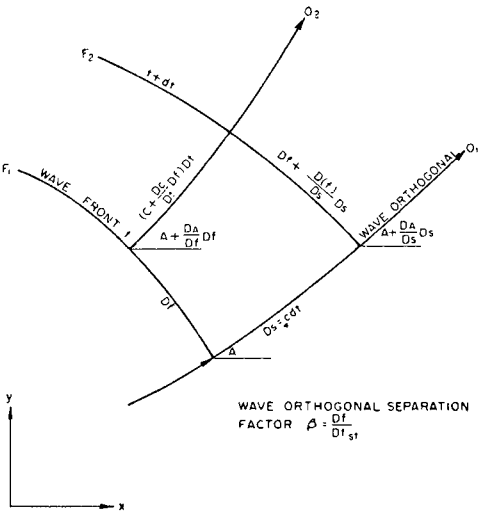

Fig. 1 Wave refraction nomenclature.

$$\dot{x} = c \cos A \tag{1}$$

$$\dot{y} = c \sin A \tag{2}$$

$$\dot{A} = \frac{dc}{dh} (h_x \sin A - h_y \sin A) \tag{3}$$

Where the subscripts on h denote a partial derivative (i.e., $h_x = \partial h/\partial x$) wave separation is determined using the following equation:

$$\ddot{\beta} + p_t \dot{\beta} + q_t \beta = 0 \tag{4}$$

where

$$p_t = -2 \frac{dc}{dh} (h_x \cos A + h_y \sin A) \tag{5}$$

$$q_t = c \frac{dc}{dh} (h_{xx} \sin^2 A - h_{xy} 2 \sin A \cos A + h_{yy} \cos^2 A) + c \frac{d^2c}{dh^2} (h_x \sin A - h_y \cos)^2 \tag{6}$$

Equations 1 through 6 are valid for both linear and cnoidal theories (14). These equations require determination of the wave speed, c, and its first and second derivatives with water depth (i.e., dc/dh, d^2c/dh^2) according to a particular wave theory. This is done readily for linear theory because one can uncouple the wave speed and wave height computations. On the other hand, the cnoidal wave speed depends on wave height and thus the wave separation factor, β. This complicates evaluation of the wave speed derivatives with depth because other variables such as wave height also vary with depth.

Linear Theory

Linear theory is used when the relative depth $d/L > .10$ or when the Ursell parameter, $U = HL^2/h^3 < 15$, (15,16). Equations for the linear wave celerity, c, and its derivatives with depth are as follows, (13):

$$c = \frac{gT}{2\pi} \tanh kh \tag{7}$$

$$\frac{dc}{dh} = \frac{c}{h} \frac{G}{1 + G} \tag{8}$$

$$\frac{d^2c}{dh^2} = - \frac{dc}{dh} \frac{2g}{c^2 (1 + G)^2} \tag{9}$$

$$G = \frac{2kh}{\sinh 2kh} \tag{10}$$

where T = wave period, h = water depth, k = wave number = $2\pi/L$, and L = wave length. Wave heights in the linear region are computed as follows:

$$H = H_o \, K_R \, K_s \tag{11}$$

where H = local wave height, H_o = the deepwater wave height, K_R = the refraction coefficient, and K_s = the shoaling coefficient. The shoaling coefficient according to linear theory is as follows:

$$K_s = \sqrt{\frac{1}{\tanh (kh) \, (1 + G)}} \tag{12}$$

Cnoidal Theory

Cnoidal theory is used when the relative depth, d/Lo <.10 and/or the Ursell parameter, U > 15. The cnoidal equations used are those reported by Svendsen and Brink-Kjaer (15). These equations represent first-order cnoidal theory.

$$c^2 = gh \left(1 + \frac{H}{h} A_c\right) \tag{13}$$

$$U = \frac{16}{3} m K^2 = \frac{HL^2}{h^3} \tag{14}$$

$$E_f = \rho g H^2 c B_c \tag{15}$$

where

$$A_c = \frac{2}{m} - 1 - \frac{3E}{mK} \tag{16}$$

$$B_c = \frac{1}{m^2} \left[\frac{1}{3} (3m^2 - 5m + 2 (4m-2) \frac{E}{K}) - (1 - m - \frac{E}{K})^2 \right] \tag{17}$$

Where m = elliptic parameter , ρ = mass density of water, K = complete elliptic integral of the first kind, E = complete elliptic integral of the second kind, and E_f = the wave energy flux. Wave speed derivatives dc/dh and d^2c/dh^2 are determined by adjusting Equations 13 through 15 for refraction and combining them to give the following:

$$\lambda = c^2 - gh - gA_c E_{fo}^{1/2} B_c^{-1/2} c^{-1/2} \beta^{-1/2} = 0 \qquad (18)$$

$$\Omega = E_{fo}^{-1/2} B_c^{-1/2} c^{3/2} \beta^{-1/2} - \frac{16}{3} K^2 \frac{h^3}{T^2}$$

$$+ \frac{16}{3} m' \frac{K^2 h^3}{T^2} = 0 \qquad (19)$$

where m' = the complementary elliptic parameter (1 - m) and E_{fo} is the reference value of energy flux. The first derivative of the wavespeed with depth, dc/dh, is determined by applying the chain rule to equations 18 and 19:

$$\lambda_h + \lambda_c \frac{dc}{dh} + \lambda_{m'} \frac{dm'}{dh} + \lambda_\beta \frac{d\beta}{dh} = 0 \qquad (20)$$

$$\Omega_h + \Omega_c \frac{dc}{dh} + \Omega_{m'} \frac{dm'}{dh} + \Omega_\beta \frac{d\beta}{dh} = 0 \qquad (21)$$

where $$\frac{d\beta}{dh} = \frac{1}{c} \frac{d\beta}{dt} (h_x \cos A + h_y \sin A)^{-1} \qquad (22)$$

The subscripts on λ and Ω denote a partial derivative e.g., $\partial\lambda_h = \partial\lambda / h$. Equations 20 through 22 are solved simultaneously for dc/dh, dm'/dh and dβ/dh. The second derivative of wave celerity with depth, d^2c/dh^2, is determined by applying the chain rule to equations 20 and 21 to give:

$$\lambda_{hh} + 2\lambda_{hc} \frac{dc}{dh} + \lambda_{hm'} \frac{dm'}{dh} + \lambda_{h\beta} \frac{d\beta}{dh} +$$

$$2\lambda_{m'c} \frac{dc}{dh} \frac{dm'}{dh} + 2\lambda_{\beta m'} \frac{d\beta}{dh} \frac{dm'}{dh} + 2\lambda_{\beta c} \frac{dc}{dh} \frac{d\beta}{dh} \qquad (23)$$

$$+ \lambda_{cc} \left(\frac{dc}{dh}\right)^2 + \lambda_c \frac{d^2c}{dh^2} + \lambda_{m'm'} \left(\frac{dm'}{dh}\right) + \lambda_{m'} \frac{d^2m'}{dh^2}$$

$$+ \lambda_{\beta\beta} \left(\frac{d\beta}{dh}\right)^2 + \lambda_\beta \frac{d^2\beta}{dh^2} = 0$$

$$\Omega_{hh} + 2\Omega_{hc}\frac{dc}{dh} + \Omega_{hm'}\frac{dm'}{dh} + \Omega_{h\beta}\frac{d\beta}{dh} +$$

$$2\Omega_{m'c}\frac{dc}{dh}\frac{dm'}{dh} + 2\,\Omega_{\beta m'}\frac{dm'}{dh}\frac{d\beta}{dh} + 2\,\Omega_{\beta c}\frac{dc}{dh}\frac{d\beta}{dh}$$

$$+ \Omega_{cc}\left(\frac{dc}{dh}\right)^2 + \Omega_{c}\frac{d^2c}{dh^2} + \Omega_{m'm'}\left(\frac{dm'}{dh}\right)^2 + \Omega_{m'}\frac{d^2m'}{dh^2} \tag{24}$$

$$+ \Omega_{\beta\beta}\left(\frac{d\beta}{dh}\right)^2 + \Omega_{\beta}\frac{d^2\beta}{dh^2} = 0$$

where

$$\frac{d^2\beta}{dh^2} = \frac{d^2\beta}{ds^2}\left(\frac{d^2h}{ds^2}\right)^{-1} \tag{25}$$

$$\frac{d^2\beta}{ds^2} = \frac{1}{c^2}\frac{dc}{dh}\left(h_x \cos A + h_y \sin A\right)\frac{d\beta}{dt} - \frac{dc}{dh}$$

$$\frac{1}{c}\left(h_{xx}\sin^2 A + h_{xy}\,2\sin A\cos A + h_{yy}\cos^2 A\right) - \tag{26}$$

$$\frac{d^2c}{dh^2}\frac{1}{c}\left(h_x \sin A - h_y \cos A\right)^2 \beta$$

$$\frac{d^2h}{ds^2} = -\sin A\frac{dA}{ds}h_x + \cos A\left(\cos A\, h_{xx} + \sin A\, h_{xy}\right)$$

$$+ \cos A\frac{dA}{ds}h_y + \sin A\left(\cos A\, h_{xy} + \sin A\, h_{yy}\right) \tag{27}$$

$$\frac{dA}{ds} = \frac{1}{c}\frac{dc}{dh}\left(\sin A\, h_x - \cos A\, h_y\right) \tag{28}$$

Equations 23 through 28 are solved simultaneously for d^2c/dh^2.

Numerical Solution of the Linear and Cnoidal Equations

The linear dispersion equation (Eq. 7) is solved by the Newton-Raphson method. The cnoidal wave equations (Eq. 13 through 15) are combined to form the cnoidal shoaling equation (15):

$$M f_1 (U) + N f_2 (U) = 1 \tag{29}$$

where

$$f_1 (U) = -B_c^{-2/3} U^{-1/3} A_c \tag{30}$$

$$f_2 (U) = B_c^{2/3} U^{4/3} \tag{31}$$

$$M = (H_r B_r L_r)^{2/3} / h^2 \tag{32}$$

$$N = M^{-1} h/gT^2 \tag{33}$$

The reference values of H_r, L_r and B_r may be given in deep water according to linear theory or in shallow according to cnoidal theory; the choice depends on where refraction computations are started. Eq. 29. is solved numerically using the Newton-Raphson Method. However, several precautions are necessary to ensure a proper solution. The Newton-Raphson procedure is formulated in terms of the complementary elliptic parameter, m', instead of the elliptic parameter, m. This is necessary because, as the elliptic parameter, m, approaches 1 (i.e., m' approaches zero), the numerical computations cannot be computed with accuracy.

The elliptic functions E and K are evaluated using the Arithmetic/Geometric Mean (AGM) scale presented in (7). The following AGM scale is used to evaluate the elliptic functions:

$$a_0 = 1 \qquad b_0 = \sqrt{m'} \qquad c_0 = \sqrt{1 - m'}$$

$$a_1 = \tfrac{1}{2} (a_0 + b_0) \qquad b_1 = \sqrt{a_0 b_0} \qquad c_1 = \tfrac{1}{2} (a_0 - b_0) \tag{34}$$

$$\text{---} \qquad \text{---} \qquad \text{---}$$

$$\text{---} \qquad \text{---} \qquad \text{---}$$

$$\text{---} \qquad \text{---} \qquad \text{---}$$

$$a_N = \tfrac{1}{2} (a_{N-1} + b_{N-1}) \qquad b_N = \sqrt{a_{N-1} b_{N-1}} \qquad c_N = \tfrac{1}{2} (a_{N-1} - b_{N-1})$$

The coefficients a_n, b_n, and c_n are computed using nine steps (N=9) which give accurate estimates (i.e. $c_9 < 10^{-6}$). From the AGM scale, E and K are computed as follows:

$$K = \pi/2a_N \tag{35}$$

$$E = K(1 - \tfrac{1}{2} (c_0 + 2c_1 + 2^2 c_2^2 + \text{---} + 2^N c_N^2)) \tag{36}$$

A second difficulty encountered in solving the cnoidal shoaling equation by the Newton-Raphson Method is that the equation has two roots (14, 15). Skovgaard and Petersen (14) conclude that the correct root corresponds to the smallest value of m' or the highest value of m. The Newton-Raphson interaction is started at a sufficiently low value of m' (i.e., $m' = 1 \times 10^{-37}$) to assure convergence to the correct root. Iterations are continued until the value of m' is determined within an accuracy of 1×10^{-6}.

The cnoidal shoaling equation describes the variation of a wave of given energy flux and wave period in the cnoidal region. Originally, Svendsen and Brink-Kjaer (15) solved the cnoidal shoaling equation assuming a continuity in energy flux between linear and cnoidal theories at the matching point of h/Lo = 0.10. However, this results in a discontinuity in wave height. Svendsen and Buhr-Hansen (16) compared the shoaling characteristics of laboratory waves to shoaling predicted by cnoidal theory and found that cnoidal theory predicted shoaling more accurately if wave height instead of wave energy is matched at h/Lo = 0.10. This presents some difficulties for wave refraction computations because there are discontinuities at the linear-cnoidal interface not only in wave height and/or wave energy, but also in wave celerity, separation, and other variables. This problem is of secondary importance for practical applications.

Numerical Solution of the Refraction Equations

The governing equations for wave refraction (i.e. 1 through 6) are solved as an initial value problem in a manner similar to Skovgaard et. at. (13). Equation 4 for the wave separation is rewritten as two first order differential equations and the governing equations are solved as a system of ordinary differential equations:

$$Z = \dot{\beta} \tag{37}$$

$$\dot{Z} = -p_t Z - q_t \beta \tag{38}$$

with the following initial conditions:

$$\begin{aligned} x &= x_o \\ y &= y_o \\ A &= A_o \\ \beta &= \beta_o \\ Z &= Z_o \end{aligned} \tag{39}$$

The integration is carried out using a combination of the Runga-Kutta-Gill and Adams-Moulton methods for initial value problems.

Evaluation of Water Depth and Water Depth Derivatives

Water depth values are stored in a bathymetry grid. The partial derivatives of water depth are computed using central difference finite difference formulas. Values of water depth (and/or its derivatives) at a point which is not on a grid point are interpolated using the following formula (4):

$$f_{i+p,\ j+q} = (1-p)\ (1-q) f_{i,j} + p(1-q)\ f_{i+1,j} + (1-p)\ q\ f_{i,j+1} + pq\ f_{i+1,\ j+1} \quad (40)$$

where i and j denote the x and y grid point respectively, and p and q define the x and y position within a grid space and f denotes the water depth and/or one of its derivatives.

Verification for Straight and Parallel Contours

Calculations were performed for straight and parallel bottom contours. The results were compared to analytical solutions based on Snell's Law. Snell's Law is expressed by the following:

$$\text{Ray Paths:}\quad \frac{\sin \alpha}{c} = \text{constant} \quad (41)$$

$$\text{Ray Separation:}\quad \beta = \frac{\cos \alpha}{\cos \alpha_o} \quad (42)$$

In the above equations α = the wave ray angle with the shore normal. The bathymetry grid for the verification runs was arranged so that α = A (the wave ray angle with the positive x-axis).

Problems in matching linear and cnoidal theories preclude complete verification of the model for straight and parallel contours. For this reason, the model was verified for the linear and cnoidal ranges separately. Accuracy of the linear portion of the model was similar to that reported by (4) and (13) for both Eq. 41 and Eq. 42. Typically, linear refraction computations deviated from Snell's Law results only about 1 part in 10,000 per time step for a variety of conditions.

The numerical model was tested in the cnoidal region for straight and parallel contours by using initial conditions appropriate for cnoidal theory. To avoid erroneous results accurate initial conditions must be specified; these values include:

x, y, A, Z, β

and $c, dc/dh, d^2c/dh^2, B_c, L, h, U, H, A_c$

The initial values for β, and Z are given by the following according to (13):

$$\beta = \frac{\cos \alpha}{\cos \alpha_{st}} \tag{43}$$

$$Z = \frac{\sin \alpha}{\cos \alpha_{st}} \left(-h_x \sin A + h_y \cos A\right) \frac{dc}{dh} \tag{44}$$

where $A = \alpha$ for the test cases, and st denotes the starting value.

Figure 2 shows the bathymetry grid, initial conditions, and wave rays for both cnoidal and linear theory for one of the test runs. In general, computational accuracy is less for cnoidal theory than linear theory. Typically, the results deviate from the Snell's Law results about 5 parts in 1000 per time step. This error stems from a variety of factors such as grid size, time step, and initial wave conditions, but primarily results from round-off error in the computation of the elliptic functions and more importantly in computation of the derivatives of the elliptic functions. Effort is presently underway to improve the accuracy of these computations. In the meantime, the verification results show the numerical scheme to be adequate for engineering applications. Uncertainties in incident wave conditions, bathymetry, and subjectivity associated in bathymetric smoothing, overshadow the small round-off error present in the model.

Fig. 2 shows that the cnoidal wave rays refract less than the linear rays, (i.e. the wave ray separation is less and the nearshore wave angle is higher for the cnoidal rays). Not evident from Fig. 2 is the fact that the cnoidal rays shoal significantly higher than the linear rays. These results are summarized in Table 1 which compares the cnoidal and linear wave rays at an equal nearshore depth. The above findings are consistent with those of Skovgaard and Petersen (14) who investigated cnoidal wave refraction over straight and parallel contours. A direct comparison to Skovgaard and Petersen (14) is not possible because computations performed for this paper were started in the cnoidal region whereas the results of Skovgaard and Petersen were related to deepwater values.

Table 1. Typical Results for Straight and Parallel Contours

Wave Characteristics at h = 2.5 feet (0.76 meters)

Theory	K_s	K_R	C feet per second (meters per second)	A (degrees)	H, feet
Linear	1.32	0.793	9.06 (2.76)	34.3	0.96 (0.29)
Cnoidal	1.56	0.787	10.25 (3.12)	38.7	1.15 (0.35)

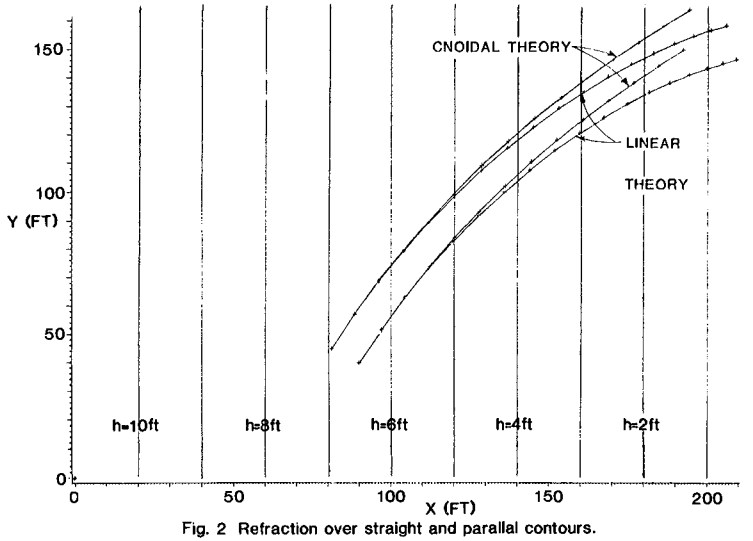

Fig. 2 Refraction over straight and parallal contours.

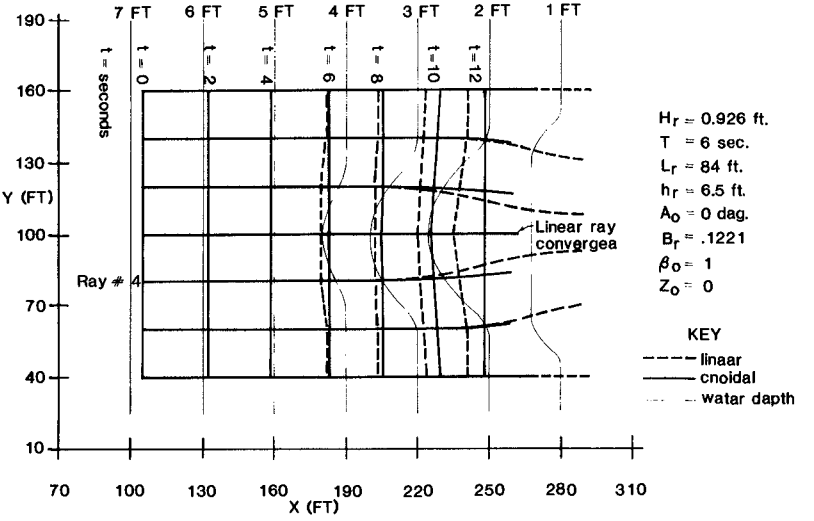

Fig. 3 Rafraction ovar an idealizad shoal.

Results For An Idealized Shoal

Refraction of cnoidal waves over an arbitrary bottom is illustrated by applying the model to an idealized shoal, similar to that used by Walker (17). The idealized shoal and bathymetry grid is shown in Fig. 3. Fig. 3 also shows the initial conditions and wave rays for a series of linear and cnoidal rays. Qualitatively, the refraction pattern for the cnoidal rays differs significantly from the linear rays as the cnoidal rays converge less over the shoal. The results are analogous to those for straight and parallel contours. Table 2 provides a comparison of linear and cnoidal results for ray number 4 at nearly equal depths. Table 2 indicates that the linear rays bend more and converge more than the cnoidal rays (i.e. higher wave angle and higher refraction coefficient). Table 2 also indicates that, despite the higher refraction coefficient for linear theory, the resulting wave height is higher for the cnoidal ray. This suggests that wave shoaling, rather than refraction, dominates the wave height growth. In summary, the cnoidal rays travel faster, propagate further, refract less, and shoal higher than linear rays.

Table 2. Typical Results For An Arbitrary Bottom

Wave Characteristics for Ray No. 4

Theory	A degrees	β	h feet (meters)	K_S	K_R	C feet per second (meters per sec.)	H, feet (meters)
Linear	8.28	0.9406	1.90 (.579)	1.42	1.031	7.75 (2.36)	1.41 (.43)
Cnoidal	3.65	0.9673	2.04 (.622)	1.85	1.017	10.38 (3.16)	1.74 (.53)

Summary

A numerical model for the refraction of linear and cnoidal waves is presented. The numerical model provides an engineering solution to the refraction of cnoidal waves. The model shows that cnoidal waves refract less and shoal higher than linear waves. Problems associated with matching linear and cnoidal theories require further research but the present model can be used until such research is available. The numerical approach is a general procedure which provides framework for incorporation of other nonlinear theories, such as third order Stokes waves in deep and intermediate water. Present effort is directed towards improving the numerical accuracy of the elliptic function and elliptic function derivatives.

The results shown in Fig. 3 for an idealized shoal are indicative of the differences between cnoidal and linear refraction for prototype applications. Clearly, nearshore waveheights based on cnoidal theory will vary considerably from those based on linear theory. This could have a considerable impact on coastal structures located in an area of divergence subjected to nonbreaking or near breaking waves. Higher nearshore wave heights and more importantly wave angles would have an impact on longshore transport calculations.

References

1. Abbott, M.B., Skovgaard, O., and Petersen, H.M., "On the Numerical Modelling of Short Waves in Shallow Water," Journal of Hydraulic Research, 16 (3), 1978.
2. Berkhoff, J.C.W., "Mathematical Models for Simple Harmonic Linear Waves; Wave Diffraction and Refraction," Delft Hydraulics Laboratory, Publication No. 163, 1976.
3. Berkhoff, J.C.W., Booy, N., and Radder, A.C., "Verification of Numerical Wave Propagation Models for Simple Harmonic Linear Water Waves," Coastal Engineering, Vol. 6, 1982, pp. 255-279.
4. Coudert, J. and Raichlen, F., discussion of "Wave Refraction near San Pedro Bay, California," by Yuan Jen, Journal of the Waterways, Harbors and Coastal Engineering Division, ASCE, Vol. 96, No. WW3, Proc. Paper 7443, Aug., 1970, pp. 737-747.
5. Crowley, J.B., Fleming, C.A., and Cooper C.K., "Computer Model for the Refraction of Nonlinear Waves," Proc. 18th Conference on Coastal Engineering, Cape Town South Africa, 1982, pp. 384-403.
6. Dean, R.G., "Evaluation and Development of Water Wave Theories for Engineering Application," Special Report No. 1, U.S. Army Corps of Engineers, Coastal Engineering Research Center, Vol. 1 and 2, 1974.
7. Goring, D.G., "Tsunamis--The Propagation of Long Waves Onto a Shelf," Report No. KH-K-83, W.M. Keck Laboratory of Hydraulics and Water Resources, California Institute of Technology, Pasadena California, 1978.
8. LeMehaute, B., and Wang, J.D., "Transformation of Monochromatic Waves from Deep to Shallow Water," U.S. Army Corps of Engineers Coastal Engineering Research Center, Technical Report No. 80-2, 1980.
9. Lillevang, O.J., Raichlen, F., Cox, J.C., and Behnke, D.L., "A Detailed Model Study of Damage to a Large Breakwater and Model Verification of Concepts for Repair and Upgraded Strength," Proc. 19th Conference on Coastal Engineering, Houston, Texas, 1984.
10. Mynet, A.E., de Voogt, W.J.P., and Schmeltz, E.J., "West Breakwater-Sines Wave Climatology," Coastal Structures Conference, Washington, D.C., 1983, pp. 17-30.
11. Munk, W.H., and Arthur, R.S., "Wave Intensity Along a Refracted Ray," Gravity Waves, National Bureau of Standards Circular 521, Washington, D.C., Nov., 1952, pp. 95-109.
12. Radder, A.C., "On the Parabolic Equation Method for Water Wave Propagation," Journal of Fluid Mechanics, 95, 1979, pp. 159-176.

13. Skovgaard, O., Jonsson, I.G., and Bertelsen, J.A., "Computation of Wave Heights Due to Refraction and Friction," ASCE Journal of the Waterways, Harbors and Coastal Engineering Division, Vol. 101, WW1, 1975, pp. 15-32.
14. Skovgaard, O. and Petersen, M. H., "Refraction of Cnoidal Waves," Coastal Engineering, Vol. 1, 1977, pp. 43-61.
15. Svendsen, I.A., and Brink-Kjaer, O., "Shoaling of Cnoidal Waves," Proc. 13th Conf. on Coastal Engineering, Vancouver, Canada, 1972.
16. Svendsen, I.A. and Buhr-Hansen, J., "The Wave Height Variation For Regular Waves in Shoaling Water," Coastal Engineering, 1, 1977, pp. 261-284.
17. Walker, J.R., "Wave Transformations over a Sloping Bottom and over a Three Dimensional Shoal," James K.K. Look Lab. of Oceanogr. Eng., Rep., 75-11. Dept. of Ocean Eng. University of Hawaii, 1974.